JOURNAL OF THERMOPHYSICS AND HEAT TRANSFER
Vol. 11, No. 1, January–March 1997

Analysis of Non-Fourier Conduction Waves from a Reciprocating Heat Source

Gary D. Mandrusiak*
General Motors Corporation, Warren, Michigan 48090-9000

The temperature profiles that result when a point heat source is swept back and forth along a rod in which heat travels at finite speed are examined. Green's functions are used to solve the hyperbolic heat equation for cases in which the source speed is half, equal to, and double, the natural thermal wave speed of the rod material. Rod temperatures are found to depend on the value of the thermal Mach number that characterizes each heating scenario. For subsonic heating, temperatures decrease smoothly ahead of the source, but drop off sharply in its wake. In supersonic heating, the temperature profile flips, moving the sharp drop in rod temperature to the source's leading edge. For transonic heating, the temperature profiles have sharp drops on both sides of the source, producing a local spike that grows with time. In all cases, the source generates three distinct wave fronts as it slides along the rod: a primary front moving with the source and two startup fronts traveling at the rod thermal wave speed. These fronts interact to produce local variations in rod temperatures that would not be predicted by Fourier's law.

Nomenclature

A_{ROD} = rod cross-sectional area, m^2
Bi = modified Biot number, $(hP_{ROD}/k)(L^2/A_{ROD})$
c = specific heat, J/kg K
c_T = material thermal wave speed, m/s
Fi = inverse Fourier number, $L^2/(\alpha\tau)$
f = heat source distribution function
h = convective heat transfer coefficient, W/m^2 K
k = thermal conductivity, W/m K
L = half-rod length, m
Ma = thermal Mach number, u/c_T
P_{ROD} = rod perimeter, m
Q = dimensionless heat flux
q = heat flux, W/m^2
q_0 = heat source intensity, W/m
T = temperature, K
t = time, s
u = forcing function speed, m/s
x = position, m
α = thermal diffusivity, m^2/s
η = dimensionless distance
θ = dimensionless temperature
ξ = dimensionless time
ρ = density, kg/m^3
σ = heat source position, m
τ = thermal relaxation time, s
Ψ = dimensionless heat source function

Introduction

MOST analyses of heat transfer in dielectric materials treat conduction as a diffusion process in which heat flux, thermal conductivity, and temperature gradient are related through Fourier's law:

$$q_x = -k\frac{\partial T}{\partial x} \tag{1}$$

With this approach, the temperature distribution in an isotropic material is governed by the familiar parabolic form of the energy equation:

$$\rho c\frac{\partial T}{\partial t} = k\frac{\partial^2 T}{\partial x^2} \tag{2}$$

Solutions to Eq. (2) imply the unrealistic notion that thermal disturbances propagate through the physical domain at infinite speed. In dielectric solids, however, thermal energy is transmitted through quanta of lattice vibrations, or phonons.[1] These lattice vibrations impose a natural relaxation time, and thus, a finite propagation speed, on conduction processes occurring within the material. Direct evidence of this finite thermal propagation speed is provided by the familiar liquid helium experiments of Bertman and Sandiford.[2] Indirect support for a finite thermal wave speed concept is also suggested by experiments on radiant heating of materials,[3] in analysis of exothermic reactions in crystals,[4] and by studies of laser heating of thin gold films.[5]

Observations like those previously noted have prompted researchers to look for a conduction model that yields more physically consistent results than those obtained using Fourier's law.[6] While the physical basis for the proposed constitutive relations has varied, each produces an energy equation in which thermal disturbances propagate at finite speed. The most common alternative to Fourier's law takes the form[7–9]

$$\tau\frac{\partial q_x}{\partial t} + q_x = -k\frac{\partial T}{\partial x} \tag{3}$$

where τ is a natural property of the material and is usually treated as constant. The speed c_T at which thermal disturbances propagate through the material is connected to the relaxation time through

$$c_T = \sqrt{k/\rho c\tau} = \sqrt{\alpha/\tau} \tag{4}$$

As c_T approaches infinity (or, equivalently, τ approaches zero), Eq. (3) correctly reduces to the familiar Fourier relationship of Eq. (1).

When used in a local energy balance, Eq. (3) yields an energy equation that is hyperbolic in form. Temperature fields obtained by solving this equation often display wavelike char-

Received March 4, 1996; revision received July 5, 1996; accepted for publication July 8, 1996.

*Staff Project Engineer, Thermal/HVAC Center, 6363 East 12 Mile Road.

acteristics that would not be predicted by traditional diffusion theory. This wave behavior is especially prominent when the thermal time scales of the situation being examined approach the material relaxation time τ. In the semiconductor industry, for example, processes used for thermal annealing[10] and material sputtering (ablation)[11] employ lasers pulsed over durations as short as 20 ns. In catalytic processes, peak heat generation rates during exothermic catalytic reactions occur as soon as 10^{-12} s after reaction initiation,[12] etc. The rapid heating rates associated with processes of this type can produce temperature profiles that include features that would not be expected from Fourier's law. The recent review article by Özisik and Tzou[13] describes many of these features, including unique reflection and transmission characteristics, sharp wave front profiles, and thermal resonance phenomena.

Material thermal response in the finite speed limit becomes particularly interesting when moving heat sources are involved. In a series of recent articles, Tzou[14–16] examines the temperature fields that result when a point source moves through a solid at constant speed. Temperature profiles derived in these studies displayed thermal shocks that would not be predicted by classical Fourier law analysis. The present study extends the domain of moving heat source problems to situations in which the thermal waves generated by the moving source are allowed to interact. The study facilitates these wave interactions by sliding a heat source back and forth along a finite rod and allowing the wave fronts it produces to collide. This heating scenario mimics that employed, for example, in a multiple-scan electron beam annealing procedure used for processing semiconductor materials.[17]

The analysis presented here solves the hyperbolic heat equation to obtain temperature profiles for cases in which the heat source speed is less than, greater than, and equal to the natural thermal wave speed of the rod. The study focuses specifically on the early-time behavior of rod temperatures during which wave effects are expected to be most pronounced. Differences between temperature profiles predicted by the hyperbolic and parabolic energy equations are identified and the impact of external cooling on rod temperatures is explored.

Problem Formulation

This study examines unsteady heat transfer in a slender rod of dimensions A_{ROD}, P_{ROD}, and $2L$ (Fig. 1). The ends of the rod are insulated and its isotropic thermal properties are assumed independent of temperature. To keep the formulation general, we assume the rod is exposed to a heat source distribution $f(x, t)$ and is cooled by convection at a rate given by Newton's law of cooling:

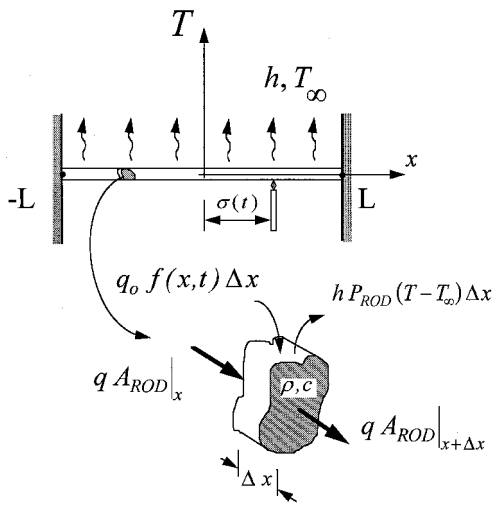

Fig. 1 Computational domain for reciprocating heat source analysis.

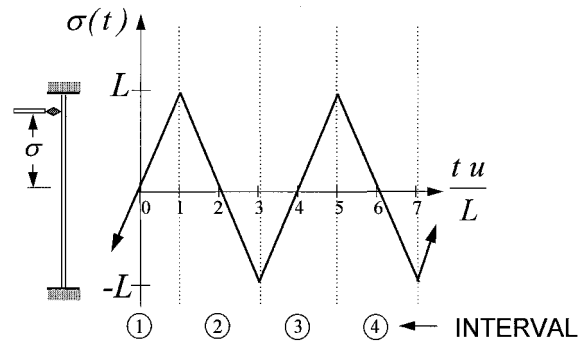

Fig. 2 Heat source position as a function of time.

$$q_{conv} = h(T - T_\infty) \tag{5}$$

Assuming temperatures are uniform across the rod cross section, a local energy balance (Fig. 1) yields the following equation governing temperatures in the rod:

$$\rho c A_{ROD} \frac{\partial T}{\partial t} = -\frac{\partial q}{\partial x} A_{ROD} - hP_{ROD}(T - T_\infty) + q_0 f(x, t) \tag{6}$$

By lumping temperatures across the rod cross section, this formulation incorporates convection effects directly into the governing equation, rather than introducing them through boundary conditions along the rod surface (cf. Ref. 18). At time zero, the rod temperature is uniform and equal to that of the ambient T_∞.

In the present study, $f(x, t)$ represents a point source of intensity q_0 applied at a location given by the position function $\sigma(t)$:

$$f(x, t) = \delta[x - \sigma(t)] \tag{7}$$

The position function that represents a point source that slides along the rod at speed u and reverses its direction at the rod endpoints (Fig. 2) is given by

$$\sigma(t) = a_m + b_m t \tag{8}$$

where the coefficients a_m and b_m for the mth oscillation interval are given by

$$\left.\begin{aligned} a_m &= 2(m-1)(-1)^m L \\ b_m &= u(-1)^{m+1} \end{aligned}\right\} \frac{(2m-3)L}{u} \le t \le \frac{(2m-1)L}{u}$$
$$m = 1, 2, 3, \ldots \tag{9}$$

To better identify the parameters that control temperatures in the rod, we recast Eqs. (3–9) in dimensionless form using the following variables:

$$\theta(\eta, \xi) \equiv k(T - T_\infty)/q_0 \qquad Q(\eta, \xi) \equiv qL/q_0 \tag{10}$$

$$\eta \equiv x/L \qquad \xi \equiv \alpha t/L^2 \tag{11}$$

With these new variables, Eqs. (3) and (6) become, respectively,

$$\frac{\partial Q(\eta, \xi)}{\partial \xi} = -Fi \frac{\partial \theta(\eta, \xi)}{\partial \eta} - Fi \cdot Q(\eta, \xi) \tag{12}$$

$$\frac{\partial \theta(\eta, \xi)}{\partial \xi} = -\frac{\partial Q(\eta, \xi)}{\partial \eta} - Bi \cdot \theta(\eta, \xi) + \Psi(\eta, \xi) \tag{13}$$

Using standard properties of the Dirac delta function,[19] the dimensionless form of $f(x, t)$ becomes

$$\Psi(\eta, \boldsymbol{\xi}) \equiv (L/A_{\mathrm{ROD}})\delta[\eta - p(\boldsymbol{\xi})] \tag{14}$$

where $p(\xi)$ is the source position function $\sigma(t)$ expressed in terms of the new variables

$$p(\xi) = A_m + B_m\xi \tag{15}$$

with

$$\left.\begin{aligned} A_m &= 2(-1)^m(m-1) \\ B_m &= (-1)^{m+1}Ma\sqrt{Fi} \end{aligned}\right\} \frac{(2m-3)}{Ma\sqrt{Fi}} \le \xi \le \frac{(2m-1)}{Ma\sqrt{Fi}}$$
$$m = 1, 2, 3, \ldots \tag{16}$$

Ma is introduced by Tzou.[14–16]

Expressions for temperature and heat flux as functions of space and time can be obtained by solving Eqs. (12) and (13) as a system.[20] Except for the simplest cases, however, it is usually easier to combine these equations into a single, second-order, partial differential equation (PDE) and solve for temperature directly. Using a series of algebraic manipulations and employing appropriate assumptions about continuity and differentiability, Eqs. (12) and (13) combine to yield the following second-order PDE for θ:

$$\frac{\partial^2\theta}{\partial\xi^2} + (Fi + Bi)\frac{\partial\theta}{\partial\xi} - Fi\frac{\partial^2\theta}{\partial\eta^2} + FiBi\theta = \frac{\partial\Psi}{\partial\xi} + Fi\Psi \tag{17}$$

As τ approaches zero, Fi approaches infinity, and Eq. (17) reduces to the familiar diffusion equation derivable from Fourier's law:

$$\frac{\partial\theta}{\partial\xi} - \frac{\partial^2\theta}{\partial\eta^2} + Bi\theta = \Psi \tag{18}$$

Boundary and initial conditions for Eq. (17) follow from the description of the rod presented earlier. In terms of the dimensionless variables defined by Eq. (10), the insulated boundary condition at the rod ends is represented by

$$Q(\pm 1, \xi) = 0 \tag{19}$$

This physics-based boundary condition can be converted to one involving temperature by integrating Eq. (13) with respect to ξ[13]

$$Q(\eta, \xi) = -Fi \cdot e^{-Fi\cdot\xi}\int_0^{\xi} e^{Fi\cdot\omega}\frac{\partial\theta(\eta, \omega)}{\partial\eta}\,\mathrm{d}\omega$$

and evaluating the result at the rod endpoints:

$$Q(\pm 1, \xi) = 0 = -Fi \cdot e^{-Fi\cdot\xi}\int_0^{\xi} e^{Fi\cdot\omega}\frac{\partial\theta(\eta, \omega)}{\partial\eta}\bigg|_{\eta=\pm 1}\mathrm{d}\omega \tag{20}$$

Since Eq. (20) must hold for all time ξ, it follows from the fundamental theorem of calculus that

$$\frac{\partial\theta}{\partial\eta}\bigg|_{\eta=-1} = 0 \qquad \frac{\partial\theta}{\partial\eta}\bigg|_{\eta=1} = 0 \tag{21}$$

for all time. The first initial condition for Eq. (17) follows from the assumed uniform rod temperature at time zero. From Eq. (10), this translates to

$$\theta(\eta, \xi)\big|_{\xi=0} = 0 \tag{22}$$

For Eq. (17) to be mathematically consistent with the physics-based, first-order, system it replaces, the second initial condition must be obtained from Eq. (13) evaluated at $\xi = 0$[21]:

$$\frac{\partial\theta}{\partial\xi}\bigg|_{\xi=0} = -\frac{\partial Q}{\partial\eta}\bigg|_{\xi=0} - Bi\cdot\theta\big|_{\xi=0} + \Psi\big|_{\xi=0}$$

Since θ and Q are both initially zero, this equation reduces to

$$\frac{\partial\theta}{\partial\xi}\bigg|_{\xi=0} = \frac{L}{A_{\mathrm{ROD}}}\delta[\eta - p(0)] \tag{23}$$

The laws of thermodynamics impose restrictions on when Eq. (3) can be combined with conventional energy conservation relationships without having to consider nonequilibrium effects.[22,23] In a recent paper,[24] a criterion was proposed for determining the conditions under which transient conduction analysis can use the energy equation in its equilibrium form. This criterion relates the magnitude of the heat flux to those of the temperature, density, specific heat, and relaxation time

$$q^2 << (\rho ck/\tau)T^2 \tag{24a}$$

or, in terms of the dimensionless groups of Eqs. (10) and (11)

$$Q^2 << (Fi)\theta^2 \tag{24b}$$

Analysis in the present study will be confined to conditions for which Eq. (24) is assumed to be satisfied.

Calculation of Rod Temperatures

Equations (17), (21), (22), and (23) govern temperatures generated in the rod by the moving source as a function of space and time. They are solved to obtain the temperature profiles using Green's functions[19]:

$$\theta(\eta, \xi) = \int_0^{\xi}\int_{-1}^{1} G(\eta, \eta_0, \xi - \xi_0)w(\eta_0, \xi_0)\,\mathrm{d}\eta_0\,\mathrm{d}\xi_0 \tag{25}$$

The Green's function $G(\eta, \eta_0, \xi - \xi_0)$ in Eq. (25) is obtained by solving Eq. (17) with homogeneous initial and boundary conditions and a right-hand side given by Dirac delta functions in space and time. Using the eigenfunction expansion technique,[25] the Green's function in this case can be shown to be

$$\begin{aligned} G(\eta, \eta_0, \xi, \xi_0) = {} & \sum_{n=0}^{n^*}\frac{e^{-D(\xi-\xi_0)}}{\sqrt{D^2 - \boldsymbol{\lambda}_n}}\cos\left[\frac{n\pi}{2}(\eta + 1)\right] \\ & \times \cos\left[\frac{n\pi}{2}(\eta_0 + 1)\right]\sinh[(\xi - \xi_0)\sqrt{D^2 - \lambda_n}] \\ & + \sum_{n=n^*+1}^{\infty}\frac{e^{-D(\xi-\xi_0)}}{\sqrt{\lambda_n - D^2}}\cos\left[\frac{n\pi}{2}(\eta + 1)\right] \\ & \times \cos\left[\frac{n\pi}{2}(\eta_0 + 1)\right]\sin[(\xi - \xi_0)\sqrt{\lambda_n - D^2}] \end{aligned} \tag{26}$$

where

$$\lambda_n = (n\pi a/2)^2 + b^2 \qquad n = 0, 1, 2, 3, \ldots \tag{27}$$

$$2D = Fi + Bi, \qquad b^2 = FiBi, \qquad a^2 = Fi \tag{28}$$

The quantity n^* denotes the highest value of n for which $D^2 > \lambda_n$. The standardizing function $w(\eta_0, \xi_0)$ for this case is given by[19]

$$w(\eta_0, \xi_0) = Fi\Psi(\eta_0, \xi_0) + \frac{\partial\Psi(\eta_0, \xi_0)}{\partial\xi_0} + \Psi(\eta_0, 0)\delta(\xi_0) \tag{29}$$

After inserting Eqs. (26–29) into Eq. (25), applying standard integration properties of the Dirac delta function,[19,26] and rearranging the terms that result, the following exact solution is obtained for the temperature distribution in the rod:

$$\theta(\eta,\xi)=\sum_{n=0}^{n^*}\frac{1}{\sqrt{D^2-\lambda_n}}(\alpha_n+\phi_n+\mu_n)\cos\left[\frac{n\pi}{2}(\eta+1)\right] + \sum_{n=n^*+1}^{\infty}\frac{1}{\sqrt{\lambda_n-D^2}}(\beta_n+\psi_n+\omega_n)\cos\left[\frac{n\pi}{2}(\eta+1)\right] \tag{30}$$

where the various coefficients in Eq. (30) are given by

$$\alpha_n = e^{-D\xi}\sinh(\xi\sqrt{D^2-\lambda_n})\cos\left(\frac{n\pi}{2}\right) \tag{31a}$$

$$\phi_n = (Fi)\int_0^{\xi} e^{-Dy}\sinh(y\sqrt{D^2-\lambda_n}) \times \cos\left\{\frac{n\pi}{2}[p(\xi-y)+1]\right\}dy \tag{31b}$$

$$\mu_n = -\left(\frac{n\pi}{2}\right)\int_0^{\xi} e^{-Dy}\sinh(y\sqrt{D^2-\lambda_n}) \times \sin\left\{\frac{n\pi}{2}[p(\xi-y)+1]\right\}\left(\frac{dp}{dy}\right)dy \tag{31c}$$

$$\beta_n = e^{-D\xi}\sin(\xi\sqrt{\lambda_n-D^2})\cos\left(\frac{n\pi}{2}\right) \tag{31d}$$

$$\psi_n = (Fi)\int_0^{\xi} e^{-Dy}\sin(y\sqrt{\lambda_n-D^2}) \times \cos\left\{\frac{n\pi}{2}[p(\xi-y)+1]\right\}dy \tag{31e}$$

$$\omega_n = -\left(\frac{n\pi}{2}\right)\int_0^{\xi} e^{-Dy}\sin(y\sqrt{\lambda_n-D^2}) \times \sin\left\{\frac{n\pi}{2}[p(\xi-y)+1]\right\}\left(\frac{dp}{dy}\right)dy \tag{31f}$$

These coefficients can be evaluated exactly (in closed form) through piecewise integration of each expression through the appropriate subintervals in Fig. 2. Numerical integration is not necessary.

In an effort to improve the convergence characteristics of the series in Eq. (30), all summations were performed using the Cesaro method.[27] Since the Cesaro method is a regular method of summability, all series that are naturally convergent yield the same result when summed with the Cesaro method. Series convergence was confirmed in each case by examining the cumulative sum as a function of the number of terms, and stopping when the result no longer changed.

Discussion of Results

The sections that follow present temperature profiles generated by exercising Eq. (30) for different values of thermal Mach number. In each case, the thermal Mach number is changed by altering u, rather than adjusting c_T or τ (cf. Ref. 28). This approach ensured that all calculations were com-

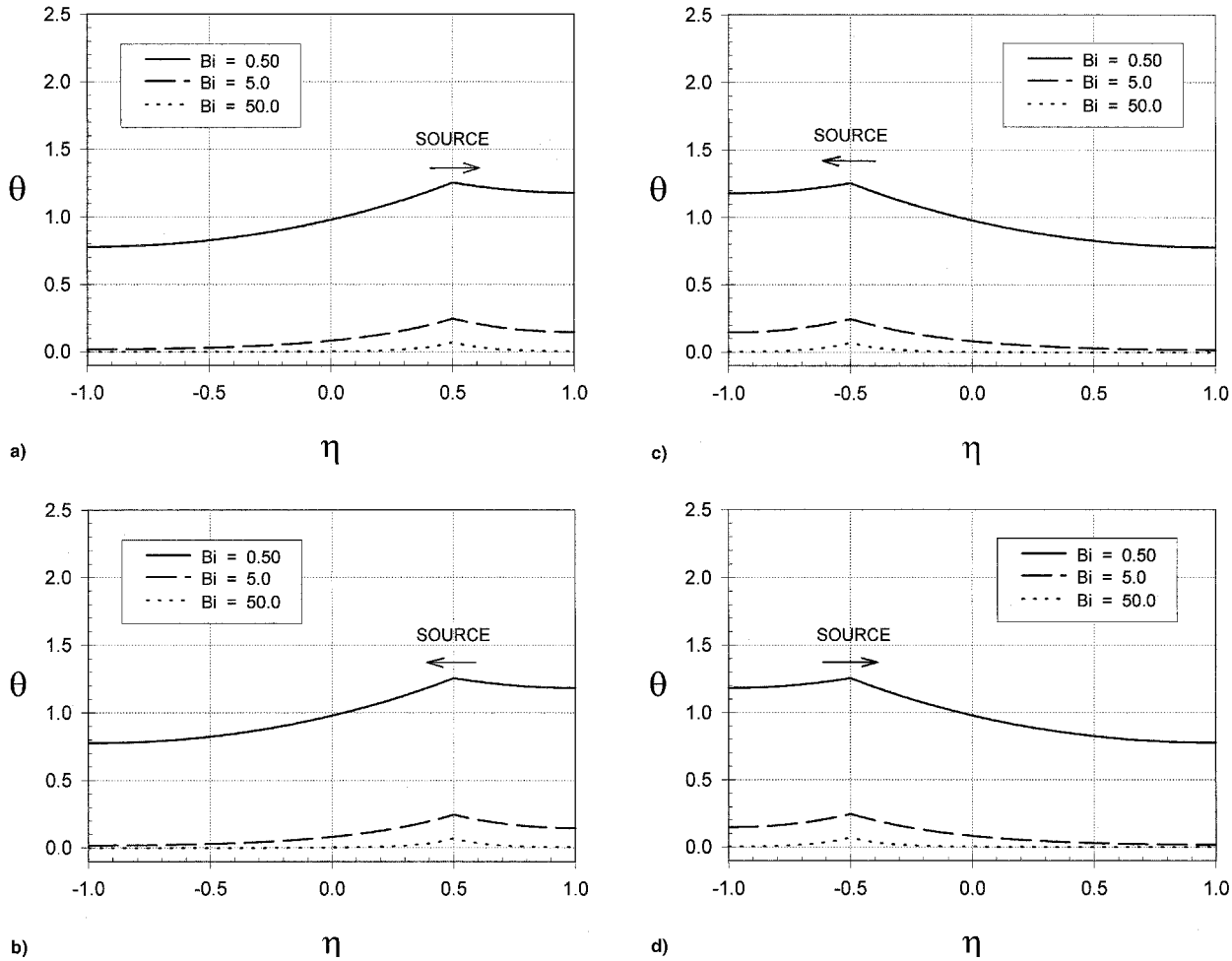

Fig. 3 Rod temperatures generated by an oscillating heat source in the diffusion limit: a) 1/8, b) 3/8, c) 5/8, and d) 7/8 cycles.

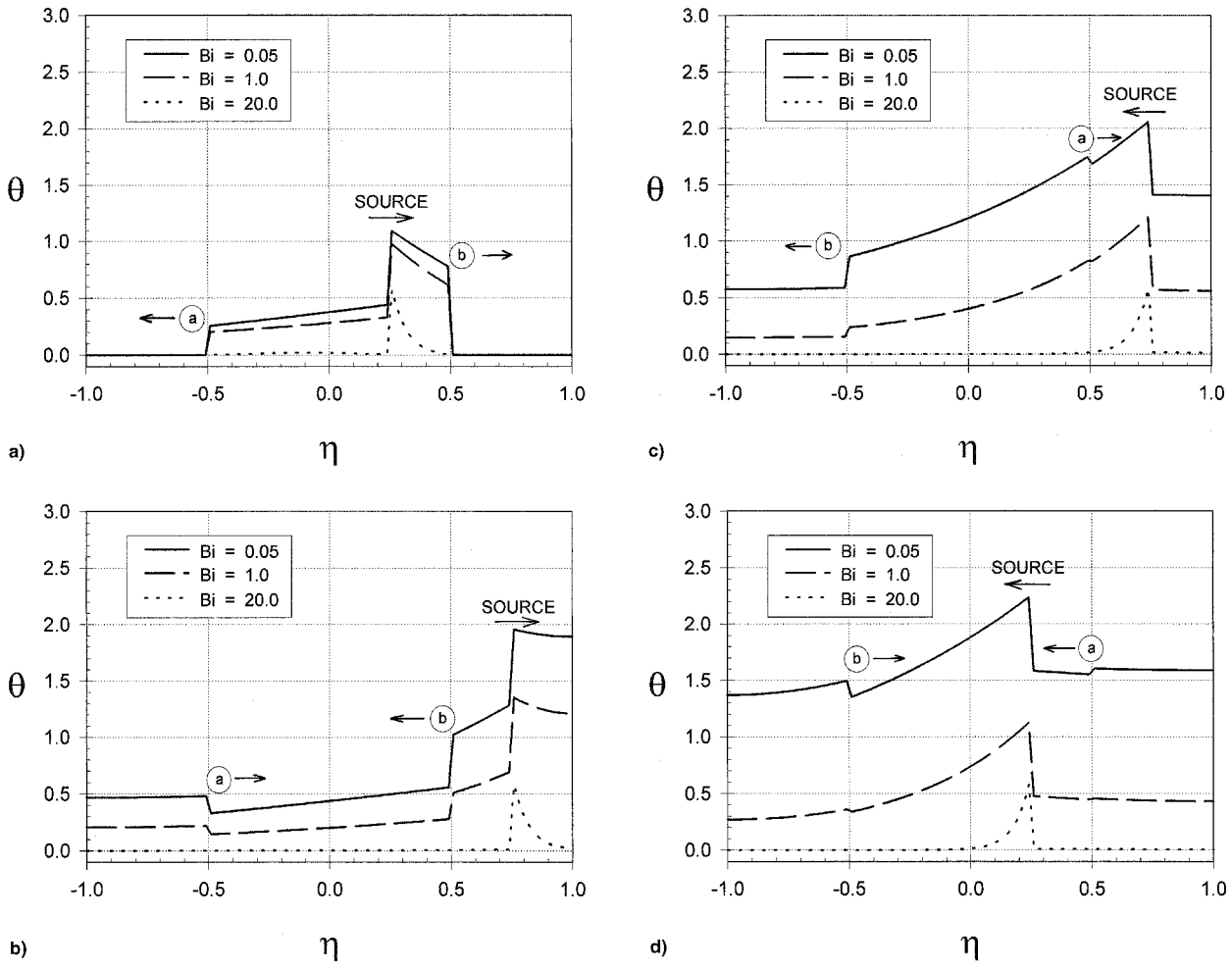

Fig. 4 Rod temperatures generated by a reciprocating heat source moving at half the natural wave speed of the rod material: a) 1/16, b) 3/16, c) 5/16, and d) 7/16 cycles.

pleted using the same value of Fi. All other parameters were selected to accentuate the effects of the finite thermal wave speed rather than to represent any particular aspect of the annealing process.[17] The thermodynamic constraint given by Eq. (24), for example, restricts analysis to conditions in which the inverse Fourier number is large. Test calculations indicated that the value of Fi primarily affected the sharpness of local maxima in the rod temperature profiles, but had little impact on profile shape. As a result, computations were performed with Fi set to 2, knowing that the general characteristics of the rod temperature profiles would still be preserved. Values used for the other problem parameters are shown on the temperature profile plots generated for each case.

Diffusion Limit ($Ma \rightarrow 0$)

Results for the diffusion limit provide a familiar baseline against which wave solutions obtained in later sections can be compared. Temperature profiles in this limiting case can be obtained by either solving Eq. (18) with boundary conditions (21) and initial condition (22), or by evaluating Eq. (30) for Ma approaching zero. If the first approach is adopted, the standard parabolic solution can be shown to be given by

$$\theta(\eta, \xi) = \frac{1}{2Bi}(1 - e^{-Bi\cdot\xi}) + \sum_{n=0}^{\infty} \gamma_n \cos\left[\frac{n\pi}{2}(\eta + 1)\right] \qquad (32)$$

where

$$\gamma_n = \int_0^{\xi} e^{-E_n y} \cos\left\{\frac{n\pi}{2}\,[p(\xi - y) + 1]\right\} dy \qquad (33)$$

with

$$E_n = (n\pi/2)^2 + Bi \qquad (34)$$

As with the coefficients in Eq. (31), γ_n can be calculated in closed form by integrating Eq. (33) piecewise through the intervals shown in Fig. 2. Although the physical implications of the second approach to generating the diffusion-limit temperature field are different, profiles provided by the low Mach number limit of Eq. (30) turn out to be identical to those provided by Eq. (32).

Figure 3 presents temperature profiles computed for the diffusion limit at four heat source positions during the first heating cycle. These profiles indicate that the highest temperature in the rod in the diffusion limit always occurs at the point where the heat source is applied. Temperatures then drop off from this maximum smoothly and continuously in both directions with no other local extrema at any point along the rod.

Subsonic Thermal Heating ($Ma = 0.5$)

Figure 4 presents rod temperatures for the case in which the source moves at half the natural thermal wave speed of the rod material. These temperature profiles differ from those in the diffusion limit (Fig. 3) in two distinct ways. First, the temperature profiles include a sharp drop immediately behind the heat source. In this area, the finite thermal relaxation time provides energy with little opportunity to extend into lower temperature regions before its source moves away. Upstream of the source, temperature profiles are similar to those seen in the diffusion limit, the only difference being the slightly steeper gradients near to where the source is applied.

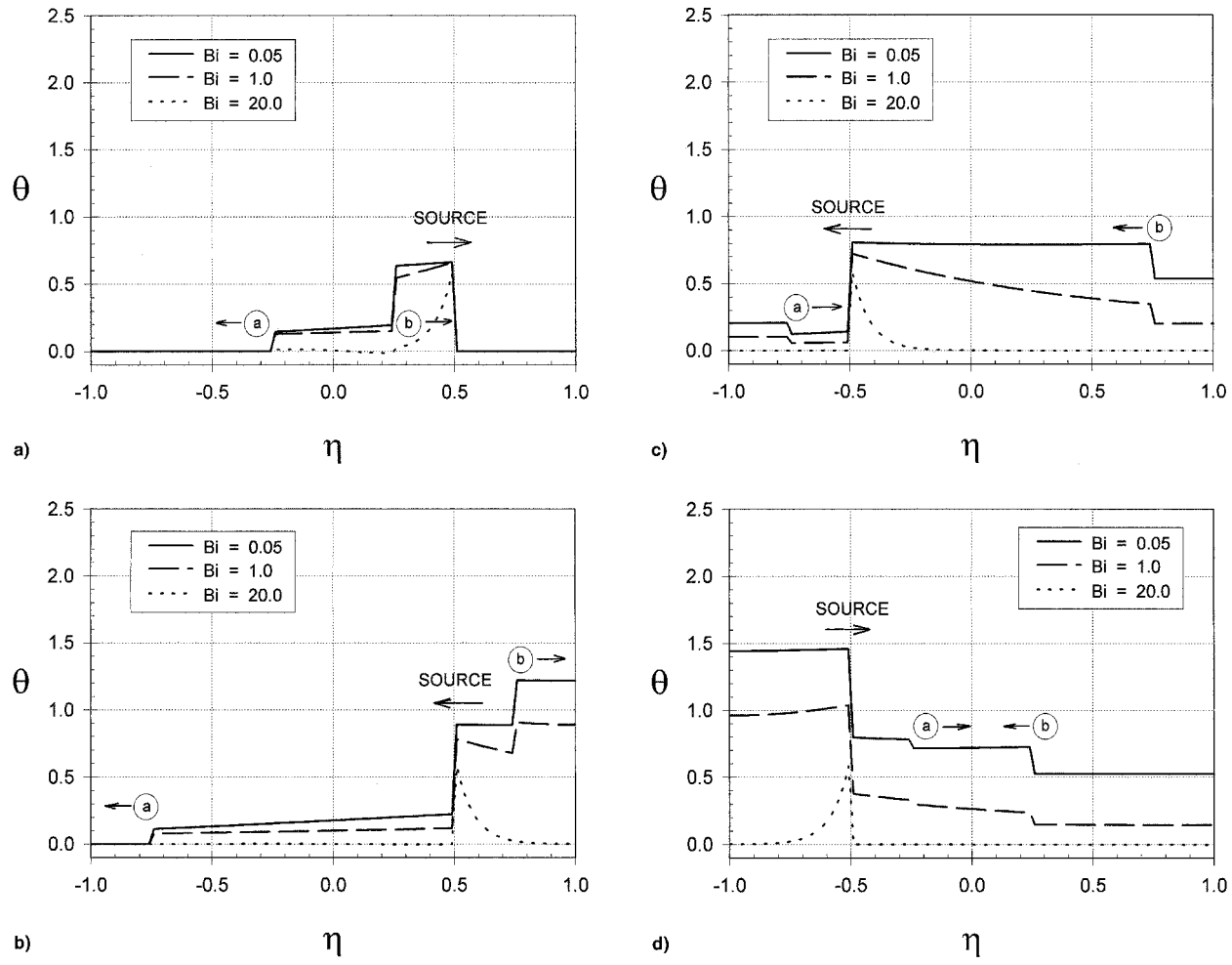

Fig. 5 Rod temperatures generated by a reciprocating heat source moving at twice the natural wave speed of the rod material: a) 1/8, b) 3/8, c) 5/8, and d) 7/8 cycles.

The temperature profiles of Fig. 4 also include two sharp wave fronts located symmetrically about the initial position of the source. These startup fronts, labeled ⓐ and ⓑ in Fig. 4, are generated the instant the heat source is energized. They travel through the rod at the natural c_T and delineate the extent to which simply activating the heat source propagates through the rod as a function of time. The character of these startup waves is similar to that of waves found in other areas of classical physics. Each, for example, preserves its shape when interacting with its counterpart traveling in the opposite direction. These interactions produce temperature levels that are consistent with both conservation of energy and standard wave superposition behavior. At the insulated rod ends, the waves and the energy they carry reflect back toward the rod center in a fashion similar to that observed by Özisik and Vick,[29] etc. Eventually, these startup fronts succumb to the effects of diffusion and convection, leaving behind temperature profiles that repeat periodically in time.

Supersonic Thermal Heating (Ma = 2.0)

Figure 5 presents rod temperatures for the case in which the source moves at twice the natural thermal wave speed of the rod material. As with the subsonic heating results in Fig. 4, the temperature profiles for Ma = 2.0 include a sharp drop in the vicinity of the heat source. In this case, however, the drop occurs immediately upstream, rather than downstream, of the point where the source is applied. In this region, active energy transport by the moving source quickly overwhelms any passive heat flow by diffusion to produce a distinct front that travels with the source.

As with the subsonic heating case considered earlier, the temperature profiles for this scenario also include two startup waves symmetrically located about the initial heat source position (labeled ⓐ and ⓑ in Fig. 5). This time, however, interactions between these startup waves and the primary source wave produce local temperatures that are decidedly different from those expected from Fourier's law. In Fig. 5b, for example, startup wave ⓑ rides over the front generated by the moving source to produce local temperatures that are higher than those found at the source. This creates the unusual circumstance, in comparison to the standard parabolic solution of Fig. 3, in which the highest temperatures along the rod do not occur at the point where the heat source is applied. One-quarter cycle later, the same startup wave reverses direction, interfering destructively with the primary wave to drop local temperatures well below those near the source (Fig. 5c). This exchange of energy between the different wave fronts continues cycle after cycle until the startup waves are consumed by convection and diffusion.

Transonic Thermal Heating (Ma = 1.0)

Figure 6 presents temperatures for the case in which the source moves at the natural thermal wave speed of the rod material. In this case, energy accumulates at the point where the source is applied to produce a local temperature spike that grows with time. This produces temperature profiles that show sharp drops both upstream and downstream of the moving source.

The temperature profiles for transonic heating also include the startup waves ⓐ and ⓑ that appeared in the other heating scenarios. Since startup wave ⓑ is always coincident with the

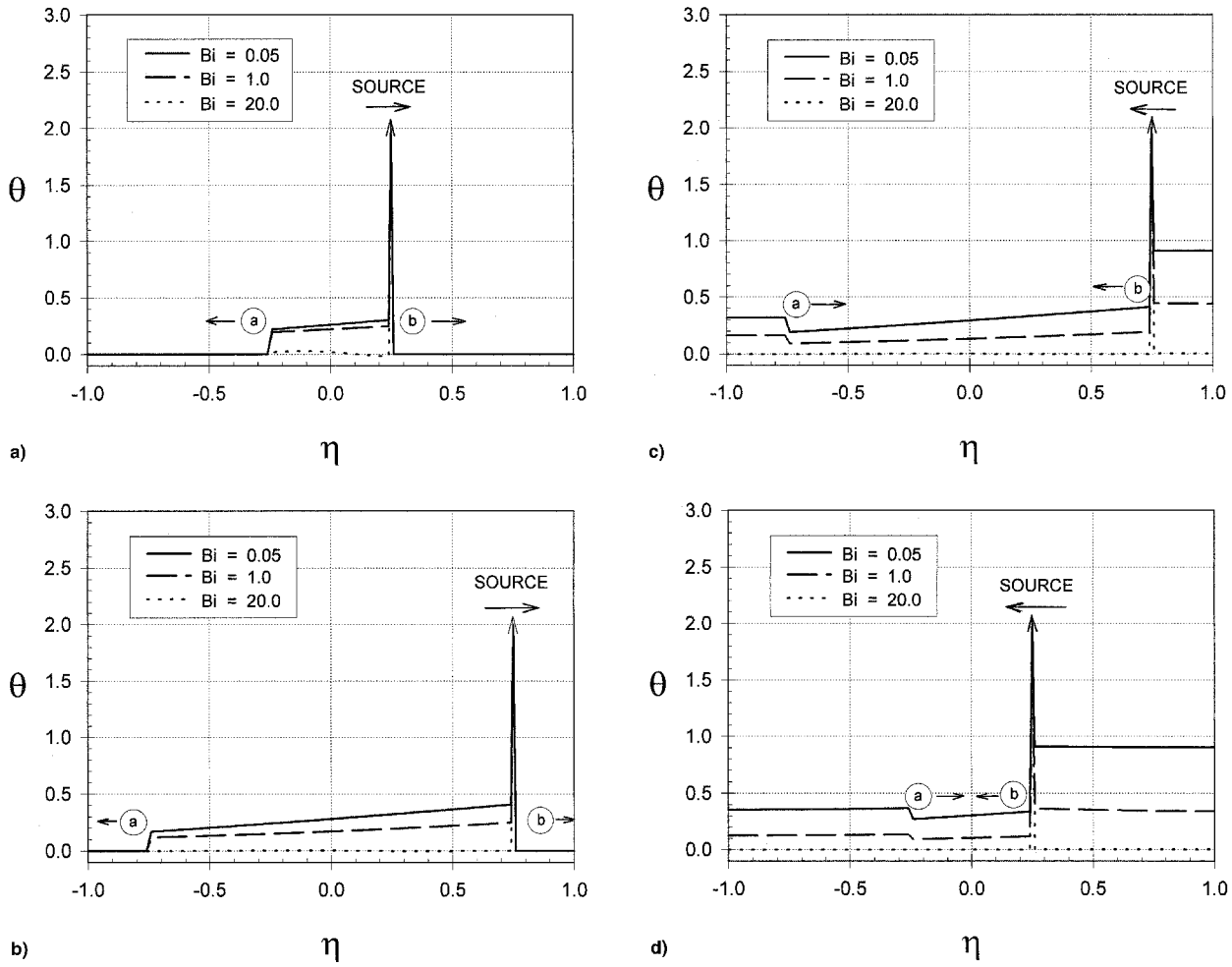

Fig. 6 Rod temperatures generated by a reciprocating heat source moving at the natural wave speed of the rod material: a) 1/16, b) 3/16, c) 5/16, and d) 7/16 cycles.

heat source, its distinct structure is buried in that of the primary wave. Startup wave ⓐ, traveling in the opposite direction at c_T, still exists, however, and behaves as it did in the subsonic and supersonic heating cases considered previously.

Influence of Convection: The Biot Number

Figures 3–6 include temperature profiles for three different values of Biot number. In each case, the Biot number is seen to control the steepness of local gradients in the rod temperature profiles, especially those near the heat source. Large Biot numbers increase the rate at which convection carries heat away from the rod, dropping temperatures to near ambient very near to where the source is applied. The coefficient of the first-order time derivative of Eq. (17) suggests that Biot number also influences how waves are damped as they move through the rod. This damping is visible in the differences in the rates at which the startup waves decay in all three heating scenarios examined.

Comparison to Thermal Resonance Studies

It is interesting to compare the heating situation examined here to that considered in the thermal resonance studies performed by Tzou.[30,31] The heating function considered in those studies had a fixed spatial distribution and an amplitude that varied periodically in time. In contrast, the heating function used here has a fixed amplitude and a spatial distribution that varies periodically with time. This difference makes it difficult to compare the response computed here to the resonance behavior explored in Refs. 30 and 31. The temperature profiles presented in the previous sections, for example, indicate that the primary wave generated by the changing spatial distribution plays a central role in determining how rod temperatures vary with space and time. Future research will search for conditions under which a reciprocating heat source can generate thermal resonance of the kind identified by Tzou.[30,31]

Concluding Remarks

This study examined the temperature profiles produced by a point heat source as it reciprocates along a rod in which heat flows at finite speed. The temperature profiles were found to vary with the value of a thermal Mach number and included two features that would not be predicted by Fourier's law:

1) A sharp drop in rod temperatures at the point where the moving heat source is applied. This drop is located immediately upstream of the moving source in supersonic heating, immediately downstream of the source for subsonic heating, and on both sides of the source for transonic heating.

2) Three distinct thermal wave fronts with positions that change as functions of time: a primary front that moves with the source, and two startup fronts that travel at the rod's natural thermal wave speed.

Convection from the surface of the rod affects both temperature gradients near the heat source and the rate at which the thermal startup waves are damped. Future work will explore the possibility of thermal resonance in this type of heating scenario and examine how the rod thermal response changes when nonequilibrium effects are considered.

Acknowledgments

The valuable feedback provided by David Stephenson, General Motors Research and Development Center, and the many insightful discussions on mathematics held with Brian Forrest,

University of Waterloo, Waterloo, Ontario, Canada, are gratefully acknowledged.

References

[1]Eckert, E. R. G., and Drake, M., *Analysis of Heat and Mass Transfer*, McGraw–Hill, New York, 1976, Chap. 2.

[2]Bertman, B., and Sandiford, D. J., "Second Sound in Solid Helium," *Scientific American*, Vol. 222, No. 5, 1970, pp. 92–101.

[3]Harrington, R. E., "Anomalous Surface Heating Rates," *Journal of Applied Physics*, Vol. 37, No. 5, 1966, pp. 2028–2034.

[4]Chan, S. H., Low, M. J. D., and Mueller, W. K., "Hyperbolic Heat Conduction in Catalytic Supported Crystallites," *American Institute of Chemical Engineers Journal*, Vol. 17, No. 6, 1971, pp. 1499–1501.

[5]Qiu, T. Q., and Tien, C. L., "Short-Pulse Laser Heating on Metals," *International Journal of Heat and Mass Transfer*, Vol. 35, No. 3, 1992, pp. 719–726.

[6]Joseph, D. D., and Preziosi, L., "Heat Waves," *Reviews of Modern Physics*, Vol. 61, No. 1, 1989, pp. 41–74.

[7]Morse, P. M., and Feshbach, H., *Methods of Theoretical Physics*, Vol. 1, McGraw–Hill, New York, 1953.

[8]Cattaneo, C., "Sur une Forme de l'Equation de la Chaleur Eliminant le Paradoxe d'une Propagation Instantanee," *Comptes Rendus Hebdom. des Seances de L'Academie des Sciences*, 1958, pp. 431–433.

[9]Chester, M., "Second Sound in Solids," *Physical Review*, Vol. 131, No. 5, 1963, pp. 2013–2015.

[10]Baeri, P., Campisano, S. U., Foti, G., and Rimini, E., "A Melting Model for Pulsing-Laser Annealing of Implanted Semiconductors," *Journal of Applied Physics*, Vol. 50, No. 2, 1979, pp. 788–797.

[11]Peterlongo, A., Miotello, A., and Kelly, R., "Laser-Pulse Sputtering of Aluminum: Vaporization, Boiling, Superheating, and Gas-Dynamic Effects," *Physical Review E: Statistical Physics, Plasmas, Fluids, and Related Interdisciplinary Topics*, Vol. 50, No. 6, 1994, pp. 4716–4727.

[12]Luss, D., "Temperature Rise of Catalytic Supported Crystallites," *Chemical Engineering Journal*, Vol. 1, 1970, pp. 311–316.

[13]Özisik, M. N., and Tzou, D. Y., "On the Wave Theory of Heat Conduction," *Journal of Heat Transfer*, Vol. 116, No. 3, 1994, pp. 526–535.

[14]Tzou, D. Y., "On the Thermal Shock Waves Induced by a Moving Heat Source," *Journal of Heat Transfer*, Vol. 111, No. 2, 1989, pp. 232–238.

[15]Tzou, D. Y., "Shock Wave Formation Around a Moving Heat Source in a Solid with Finite Speed of Wave Propagation," *International Journal of Heat and Mass Transfer*, Vol. 32, No. 10, 1989, pp. 1979–1987.

[16]Tzou, D. Y., "Thermal Shock Phenomena Under High Rate Response in Solids," *Annual Review of Heat Transfer*, edited by Chang-Lin Tien, Vol. 4, Hemisphere, Washington, DC, 1991, Chap. 3.

[17]Shah, N. J., McMahon, R. A., Williams, J. G. S., and Ahmed, H., "Multiple-Scan E-Beam Method Applied to a Range of Semiconductor Materials," *Laser and Electron Beam Solid Interactions and Materials Processing*, edited by J. F. Gibbons, L. D. Hess, and T. W. Sigmon, Elsevier North–Holland, New York, 1981, pp. 201–208.

[18]Glass, D. E., Tamms, K. K., and Railkar, S. B., "Hyperbolic Heat Conduction with Convection Boundary Conditions and Pulse Heating Effects," *Journal of Thermophysics and Heat Transfer*, Vol. 5, No. 1, 1991, pp. 110–116.

[19]Butkovskii, A. G., *Green's Functions and Transfer Functions Handbook*, Wiley, New York, 1980, Chap. 1.

[20]Koshlyakov, N. S., Smirnov, M. M., and Gliner, E. B., *Differential Equations of Mathematical Physics*, North–Holland, Amsterdam, 1964, Chap. 11.

[21]Zachmanoglou, E. C., and Thoe, D. W., *Introduction to Partial Differential Equations with Applications*, Williams and Wilkins, Baltimore, MD, 1976, p. 378.

[22]Kaliski, S., "Wave Equation of Heat Conduction," *Bulletin of the Polish Academy of Science*, Vol. 13, No. 4, 1965, pp. 211–219.

[23]Coleman, B. D., Fabrizio, M., and Owen, D. R., "On the Thermodynamics of Second Sound in Dielectric Crystals," *Archive for Rational Mechanics and Analysis*, Vol. 80, No. 2, 1982, pp. 135–158.

[24]Vedavarz, A., Kumar, S., and Karim Moallemi, M., "Significance of Non-Fourier Heat Waves in Conduction," *Journal of Heat Transfer*, Vol. 116, No. 1, 1994, pp. 221–224.

[25]Zauderer, E., *Partial Differential Equations of Applied Mathematics*, 2nd ed., Wiley, New York, 1983, Chap. 7.

[26]Lowan, A. N., "On Transverse Oscillations of Beams Under the Action of Moving Variable Loads," *The London, Edinburgh, and Dublin Philosophical Magazine and Journal of Science*, Vol. 19, No. 127, 1935, pp. 708–715.

[27]Spiegel, M. R., *Advanced Calculus*, McGraw–Hill, New York, 1963, p. 233.

[28]Glass, D. E., and McRae, D. S., "Variable Specific Heat and Thermal Relaxation Parameter in Hyperbolic Heat Conduction," *Journal of Thermophysics and Heat Transfer*, Vol. 4, No. 2, 1990, pp. 252–255.

[29]Özisik, M. N., and Vick, B., "Propagation and Reflection of Thermal Waves in a Finite Medium," *International Journal of Heat and Mass Transfer*, Vol. 27, No. 10, 1984, pp. 1845–1854.

[30]Tzou, D. Y., "Damping and Resonance Characteristics of Thermal Waves," *Journal of Applied Mechanics*, Vol. 59, No. 4, 1992, pp. 862–867.

[31]Tzou, D. Y., "Thermal Resonance Under Frequency Excitations," *Journal of Heat Transfer*, Vol. 114, No. 2, 1992, pp. 310, 316.